# CHARACTERIZATION OF THE SUBCLINICAL PERILESIONAL ZONE IN THE MACULA OF EARLY-STAGE ABCA4 DISEASE

A PREPRINT

**Aiden Zee**[ab], **Winston Lee**[b*], **Pei-Yin Su**[b], **Jana Zernant**[b], **Stephen H. Tsang**[bc], **Rando Allikmets**[bc*]

[a]Cypress Bay High School, Weston, FL USA

[b]Department of Ophthalmology, Columbia University Irving Medical Center, New York, NY, USA

[c]Department of Pathology & Cell Biology, Columbia University Irving Medical Center, New York, NY, USA

[*]Correspondence: wl2355@cumc.columbia.edu, rla22@cumc.columbia.edu

Hammer Health Sciences Building, Columbia University College of Physicians and Surgeons

701 W 168th St, New York, NY 10032

November 16, 2024

## ABSTRACT

Purpose: To characterize photoreceptor layer thinning in clinically unremarkable regions adjacent to the atrophic lesion in early-stage ABCA4 disease eyes. Methods: 27 patients with confined atrophic lesions ($\leq$ 3.5mm in diameter) were included. Two pathogenic alleles were confirmed by sequencing of the *ABCA4* locus. Multimodal imaging included color fundus photography, short wavelength-autofluorescence (SW-AF) and near infrared-autofluorescence (NIR-AF) imaging. Total receptor+ (TREC+) thickness was segmented in spectral domain-optical coherence tomography (SD-OCT) scans in patient eyes (n=27) along with age-matched healthy control eyes (n=20). Results: $\mu_{age}$ of the study cohort was 24.1 years and 15/27 (55.6%) patients harbored genotypes consisting of the p.(Gly1961Glu) variant in *ABCA4*. Atrophic lesions in the central macula ranged from 0.61 to 3.13 mm in diameter ($\mu$ = 1.73, $\sigma$ = 0.70). Six patients had mild RPE mottling adjacent to the lesion on NIR-AF. The atrophic lesion corresponded to a disruption of photoreceptor-attributable bands on SD-OCT while all layers were visibly intact outside the lesion. TREC+ thickness in patient eyes were <0.15 mm or below $4\sigma$ of normal control eyes immediately adjacent to the lesion edge and gradually normalized to within $\pm$ $2\sigma$ at $\approx$ 1.2 mm eccentricity from the fovea. Conclusion: A uniform subclinical perilesional zone (SPZ) of photoreceptor thinning extends around the perimeter of early-stage atrophic lesions in ABCA4 disease. This region spatially maps to known regions of vision loss and more accurately approximates the extent of photoreceptor abnormality compared to the disease changes visible on standard fundus imaging. Translational relevance: Semi-automated segmentation of SD-OCT scans identifies a consistent subclinical biomarker relevant to early photoreceptor degeneration in ABCA4 disease.

***Keywords*** ABCA4, Stargardt disease, atrophy, sub-clinical, photoreceptors, OCT

# 1 Introduction

Pathogenic variation in the *ABCA4* gene (MIM♯ 601691) is the underlying cause[1] of several retinal degenerative disorders including Stargardt disease,[74] fundus flavimaculatus,[16, 21, 23, 24] cone-rod dystrophy (CRD),[22, 49] rapid-onset chorioretinopathy (ROC),[83] late-onset maculopathy,[42, 62, 61, 95, 94] among many others.[13] Each of these disorders is characterized by the progressive degeneration of photoreceptors, specialized light-sensitive cells in the retina responsible for vision. The ABCA4 protein plays a crucial role in the visual cycle by transporting byproducts, specifically N-retinylidene-PE,[3] out of photoreceptors and into retinal pigment epithelium (RPE) cells. Impaired ABCA4 function impedes this clearance process resulting in the irreversible formation and subsequent accumulation[6, 11] of cytotoxic bisretinoids (lipofuscin) that trigger the death of both the RPE photoreceptor layers in the retina.[73, 69, 70]

Clinically, this degenerative process manifests as an atrophic lesion in the central macula that expands outwardly from the fovea over time resulting in further deterioration of central vision.[13] While the size of the atrophic lesion in the retina generally correlates with the severity of vision loss, prior studies have found that the outer boundary of the dense scotoma (blind spot) typically extends beyond the visible edge of the atrophic lesion in the fundus—a finding that is unique to ABCA4 disease as compared to other macular disorders such as dry age-related macular degeneration (AMD).[56, 81] Consistent with this phenomenon, fixation studies have shown that the eccentric preferred retinal locus (PRL) in ABCA4 disease eyes is located far away from the edge of the atrophic lesion.[27, 59, 64, 65, 86] Furthermore, clinically unremarkable regions adjacent to the atrophic lesion have also been shown to exhibit reduced visual sensitivity by psychophysical tests such as fundus-driven perimetry [4, 10, 80, 79] and decreased electrophysiological function on multifocal electroretinogram (mfERG) recordings.[39, 40, 66]

Although early functional attenuation in otherwise "clinically unremarkable" areas of the fundus has been observed in ABCA4 disease,[2, 85] more sophisticated imaging techniques have nevertheless revealed that these areas in fact do exhibit disease-related structural changes. Optical coherence tomography (OCT) is a non-invasive imaging technique that captures high-resolution, cross-sectional images of the retina, allowing for detailed visualization of its layers and detection of subtle structural changes in eye diseases.[29] Lesions marked by outer retinal atrophy in the fundus correspond to the loss or disruption of photoreceptor- and RPE-attributable layers visible on individual B-scans. While these layers are generally intact in clinically unremarkable areas, several studies have shown that they exhibit significant thinning compared to healthy eyes.[25, 57, 38, 41, 50, 52, 57, 67, 78, 88] Retinal layer thinning is a commonly recognized precursor stage to atrophy in both patients and animal models of ABCA4 disease,[28, 47, 56, 72] making it a valuable biomarker for tracking disease progression and evaluating clinical trial outcomes. Characterizing retinal layer thinning in ABCA4 disease in a consistent manner, however, has been challenging due to its profound clinical heterogeneity.[13] To accommodate this heterogeneity, most prior studies have focused on broad averaging approaches (comparing fixed regions and ETDRS grids)[25, 26, 38, 50, 52, 67, 78, 88, 89] that obscure localized variations which may be insightful to disease progression. To make better use of retinal layer thinning as a reliable biomarker in the clinic and clinical trials, a more incisive approach focusing on localized and consistent changes relative to specific disease patterns is necessary.

The aim of this study is to characterize localized changes in photoreceptor layer thickness in areas adjacent to atrophic lesions in ABCA4 disease. To minimize the effect of variable disease features that may confound thickness measurements (e.g., the presence of yellow, pisciform flecks[14, 71], QDAF,[75] etc.) study inclusion was limited to early-stage patients/eyes with confined atrophic lesions and no other visible surrounding (extra-lesional) disease alterations in the fundus.

# 2 Materials & Methods

## 2.1 Ethics approval

All study subjects were consented before participation under the protocol #AAAI9906 approved by the Institutional Review Board at Columbia University Irving Medical Center. All study-related procedures adhered to the tenets established by the Declaration of Helsinki.

## 2.2 Clinical examination

Complete ophthalmic examinations were provided by a retinal specialist, which included a slit-lamp and dilated fundus examination. Color fundus photographs (30° and 50° magnification) were captured using the FF450plus Fundus Camera (Carl Zeiss Meditec). Fundus autofluorescence images (both short wavelength-autofluorescence (SW-AF, 488-nm excitation) and near infrared-autofluorescence (NIR-AF, 787-nm excitation)), and high-resolution spectral-domain

optical coherence tomography (SD-OCT) scans were acquired using a Spectralis HRA+OCT (Heidelberg Engineering, Heidelberg, Germany).

### 2.3 Molecular screening

All causal genetic variants were identified by either direct sequencing of the *ABCA4* locus or whole-exome sequencing as previously described.[92, 93] All detected possibly disease-associated variants were confirmed by Sanger sequencing and determined to be pathogenic through multiples lines of evidence (Supplemental Table S1). Variants identified from sequencing were annotated with established pathogenicity prediction scores, including phyloP100,[58] M-CAP (percentile range 0 to 1),[32] REVEL (likelihood ratio 0 to 1),[30] CADDv1.6 (PHRED scale 0 to 48),[37, 60] DANN, Eigen (probability score -4.09 to 6.31),[31] SpliceAI ($\Delta$score)[33] and Pangolin ($\Delta$score),[91] using ANNOVAR.[87] Minor allele frequences (MAF) were obtained from the gnomAD database v3.1.2 (`https://gnomad.broadinstitute.org/gene/ENSG00000198691?dataset=gnomad_r4`) (assessed August 2024). Finally, the phase of all variants were either confirmed by parental screening or imputed based on co-occurrence in the general populations (`https://gnomad.broadinstitute.org/variant-cooccurrence`).

### 2.4 Outer retinal layer segmentation on SD-OCT

Retinal layer thicknesses were obtained by segmenting single 9-mm high resolution SD-OCT scans through the fovea in a single, randomly selected eye from each patient and 20 age-matched, healthy control eyes (Supplemental Figure S1). Total receptor+ (TREC+) was defined as the distance between the Bruch's membrane/choroid interface and the inner nuclear layer (INL)/outer plexiform layer (OPL) boundary (Supplemental Figure S2).[28] The boundaries of TREC+ were measured manually using the caliper tool in the HEYEX software (Heidelberg Engineering, Heidelberg, Germany). The thickness of TREC+ was measured at 0.5 mm interval positions (13 positions total) along the temporal and nasal meridian from the fovea (origin). In plots, all thickness profiles are represented as right eyes.

### 2.5 Statistical analyses

Statistical analyses and plots (mean of grader measurements) were performed using a custom written program in R (https://www.r-project.org) through RStudio (https://www.rstudio.com). SD-OCT measurements were performed by two independent graders (AZ and WL) along with a third adjudicator when necessary (PYS). Intraclass correlation coefficients (ICC), calculated using the irrICC package (https:// cran.r-project.org), showed excellent intergrader agreement for patients (ICC>0.9818) and controls (ICC>0.9997). Comparison of non-normal distributions (e.g. age at examinaation, fundus measurements) were based on unpaired, two-tailed P-values from Mann-Whitney U test. Wilcoxon signed rank test for paired data was used oo test the symmetry of values from the same eye across patients (e.g., temporal and nasal SPZ width). Contingency tables (2x2) were compared using both a Fisher's exact test and Chi-square test with Yate's correction.

## 3 Results

### 3.1 Clinical examination and genetic screening

Twenty-seven patients with confined atrophic lesions and no other surrounding disease alterations in the macula detected on fundus examination were included in the study (Figure 1). Considering the imaging field of the testing modalities (see Methods), patients/eyes with lesions with diameters of >3.5 mm (area $\approx$10 $mm^2$) were excluded to ensure that an adequate area of the adjacent fundus was available for analysis. Demographic, clinical and genetic characteristics of the study cohort are summarized in Table 1. Cohort age ranged from 11-65 years; mean ($\mu$) = 24.1 years, standard deviation ($\sigma$) = 12.0 years.

### 3.2 Sequencing and analysis of *ABCA4*

All patients were biallelic for known or expected disease-causing variants in *ABCA4*. Phase was confirmed by familial segregation in all except 4 patients (P16, P23, P24 and P26); phasing in the latter was statistically imputed based on co-occurrence in gnomAD (Supplemental Figure S3). Thirty-three unique variants were identified across the cohort: 17 missense, 5 complex alleles, 2 nonsense, 5 intronic substitutions, 3 deletions and 1 duplication. Predicted in silico or established pathogenicity evidence for each unique variant are summarized in Supplemental S1. The phenotype selected in this study is consistent with the clinical diagnosis of bull's eye maculopathy (BEM), an entity associated with the frequent p.(Gly1961Glu) mutation.[8] As expected, therefore, the majority of genotypes in this study cohort

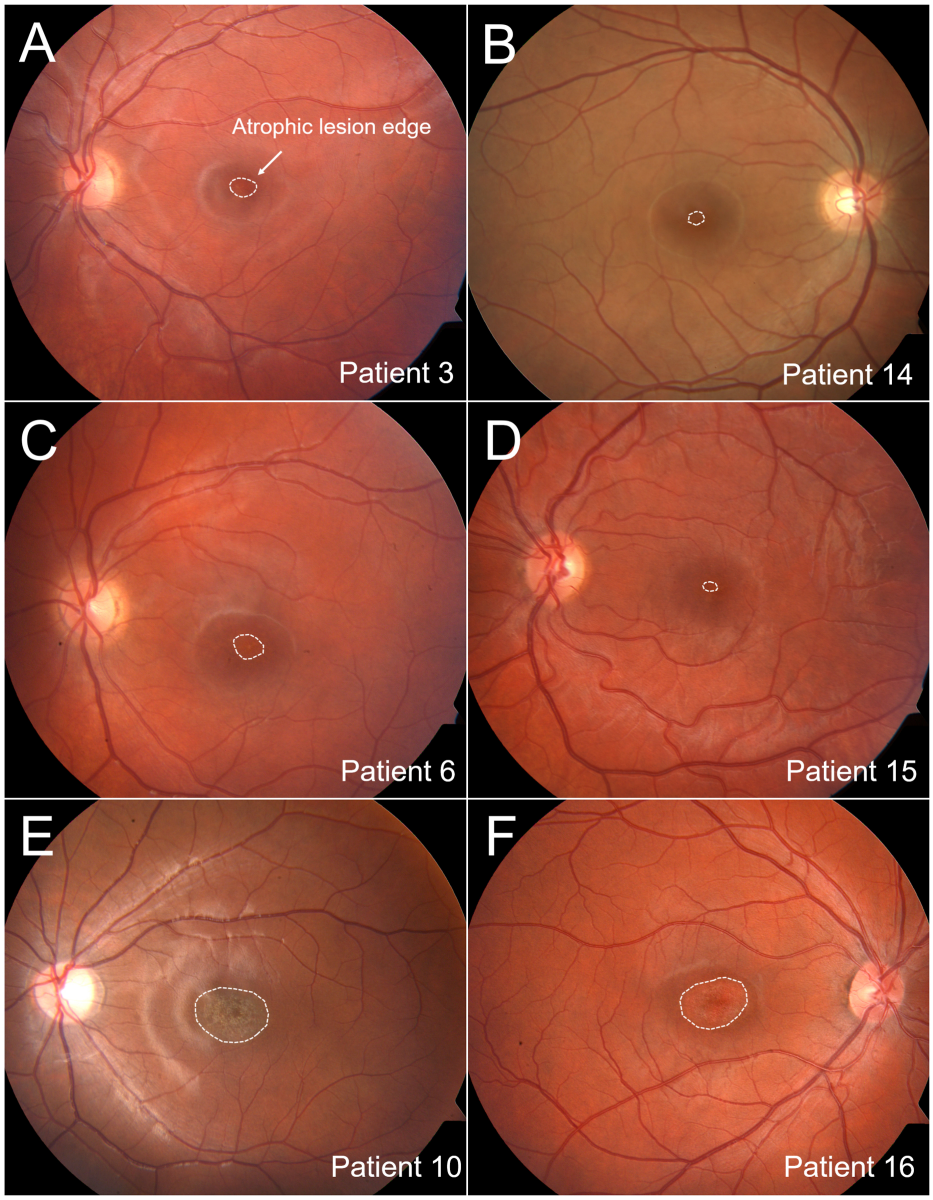


Figure 1: Color fundus photographs showing the confined atrophic lesion and clinically unremarkable periphery of the (A) left eye of Patient 3, (B) right eye of Patient 14, (C) left eye of Patient 6, (D) left eye of Patient 15, (E) left eye of Patient 10 and (F) right eye of Patient 16. The white dotted line delineates the visible edge of each atrophic lesion.

(15/27 patients, 56%) consisted of the p.(Gly1961Glu) variant. Notably, four of the p.(Gly1961Glu) alleles harbored additional variants in cis: three with the deep intronic c.769-784C>T modifier[43, 61, 63] (P19, P24 and P27) and one with the p.(Thr1253Met) coding variant (P23).

### 3.3 Multimodal fundus autofluorescence (FAF) imaging

The atrophic lesion observed on fundoscopy appeared as a dark region on both fundus autofluorescence modalities (Figure 2). On short wavelength-autofluorescence (SW-AF, 488-nm excitation), the central hypoAF region exhibited a heterogeneous (punctate) appearance in most eyes (38/54 eyes, 70%) and was surrounded by a hyperAF border in 28 eyes (52%). Comparatively, the central hypoAF lesion exhibited a more homogeneous appearance on near infrared -autofluorescence (NIR-AF, 787-nm excitation). On both modalities, no significant disease-associated abnormalities

Table 1: Demographic, clinical and genetic characteristics of the study cohort.

| Patient | BCVA OD | BCVA OS | *ABCA4* allele 1 | *ABCA4* allele 2 |
|---|---|---|---|---|
| 1 | 20/25 | 20/100 | p.([Leu541Pro;Ala1038Val]) | p.(Leu2027Phe) |
| 2 | 20/150 | 20/150 | c.5196+1G>A | p.(Leu2027Phe) |
| 3 | 20/150 | 20/100 | p.(Trp821Arg) | p.(Cys2150Tyr) |
| 4 | 20/20 | 20/25 | p.(Gly1961Glu) | p.(Val615Ala) |
| 5 | 20/150 | 20/150 | p.(Val989Ala) | c.2918+5G>A |
| 6 | 20/125 | 20/100 | p.(Gly1961Glu) | p.(Pro1380Leu) |
| 7 | - | - | p.([Leu541Pro;Ala1038Val]) | p.(Gly1961Glu) |
| 8 | 20/25 | 20/40 | p.(Thr1112Asn) | p.([Gly863Ala;Asn1868Ile]) |
| 9 | 20/150 | 20/150 | c.[5461-10T>C;5603A>T] | p.(Arg1098Cys) |
| 10 | 20/100 | 20/150 | p.(Gly1961Glu) | p.(Phe2161Cysfs*3) |
| 11 | 20/150 | 20/150 | p.(Gly1961Glu) | p.(Ala1773Val) |
| 12 | 20/100 | 20/80 | p.(Val1682_Val1686del) | p.(Gly1961Glu) |
| 13 | 20/50 | 20/40 | c.4253+4C>T | p.(Arg2107His) |
| 14 | 20/40 | 20/80 | p.(Gly1961Glu) | p.(Gln1412*) |
| 15 | 20/50 | 20/100 | p.(Gly1961Glu) | p.(Met1733Valfs*2) |
| 16 | 20/80 | 20/80 | p.(Ser84Thrfs*16) | p.(Arg2107His) |
| 17 | 20/60 | 20/70 | p.(Gly1961Glu) | p.(Trp15*) |
| 18 | 20/20 | 20/20 | p.(Arg212Cys) | p.(Gly1961Glu) |
| 19 | 20/100 | 20/100 | p.([Leu257Aspfs*3,Gly1961Glu]) | p.(Cys2150Arg) |
| 20 | 20/100 | 20/150 | p.(Gly991Arg) | p.(Leu1138His) |
| 21 | 20/30 | 20/30 | p.(Glu1022Gly) | p.(Gly1961Glu) |
| 22 | 20/30 | 20/30 | p.(Gly1961Glu) | c.4947delC |
| 23 | 20/80 | 20/70 | c.3050+5G>A | p.([Thr1253Met;Gly1961Glu]) |
| 24 | 20/40 | 20/50 | p.([Leu257Aspfs*3,Gly1961Glu]) | p.(Pro1380Leu) |
| 25 | 20/100 | 20/100 | p.(Gly1961Glu) | p.(Gly1961Glu) |
| 26 | 20/50 | 20/50 | p.(Gly1961Glu) | p.(Arg1129Cys) |
| 27 | CF | CF | p.([Leu257Aspfs*3,Gly1961Glu]) | p.(Gly1961Glu) |

were detected beyond the lesion boundary except in a subgroup of 6 patients (P1, P8, P13, P19, P23 and P24) in whom mild RPE mottling immediately adjacent to the lesion border was visible on NIR-AF (Figure 2C and Figure 22D).

### 3.4 Spectral-domain optical coherence tomography (SD-OCT)

Within the atrophic lesion, several outer retinal layers were visibly disrupted—specifically, the outer retinal layer (ONL), external limiting membrane (ELM) and the ellipsoid zone (EZ) band on SD-OCT (Figure 3). Comparative analysis between FAF and SD-OCT confirmed that the horizontal diameter of the atrophic lesions on both SW-AF and NIR-AF images (Figure 2, dashed vertical lines) spatially corresponds best with the horizontal diameter of EZ loss.[17, 35, 53, 55] The mean horizontal diameter of EZ loss in all study eyes was 1.76 mm ($\sigma$ = 0.70, 0.61-3.13 mm) (Table 2). Although all outer retinal layers adjacent to the atrophic lesion were present and intact, several visible abnormalities were noted in this region. In all study eyes, the ELM was visibly thickened[36, 44] and the interdigitation zone (IZ)[34] was visibly indiscernible between the EZ and RPE layers (Figure 3, insets). In both eyes of 20/27 patients (74%), hyper-reflective foci were observed between the ELM and outer plexiform layer (OPL).[9] Most notably, this entire region appeared to be abnormally thin, particularly the ONL and other photoreceptor-attributable layers, relative to healthy eyes (Figure 3).

### 3.5 Photoreceptor layer thickness quantification

To quantify the extent of photoreceptor-attributable layer thinning, the thickness of total receptor+ (TREC+), defined as the distance between the Bruch's membrane(BM)/choroid(Ch) interface and the inner nuclear layer (INL)/OPL boundary[28] (Supplemental Figure S2), was segmented in all patients (27 eyes) and compared to 20 age-matched, healthy control eyes (Supplemental Table S1) (Supplemental Figure S1). On average, TREC+ thickness fell below -2$\sigma$ approximately 1.5 - 2.0 mm on both the temporal nasal sides of the EZ lesion (Figure 4A) (Table 2). Significant thinning was most pronounced in immediately adjacent areas and gradually normalized (to within ±2$\sigma$ of healthy eyes) with increasing eccentricity. TREC+ thickness in all study eyes were below 4$\sigma$ of healthy eyes at ≈0.5 mm from the EZ lesion (Figure 4B). At 1.0 mm eccentricity, significant thinning was still found in 13/27 (48%) study eyes, and at 2.0

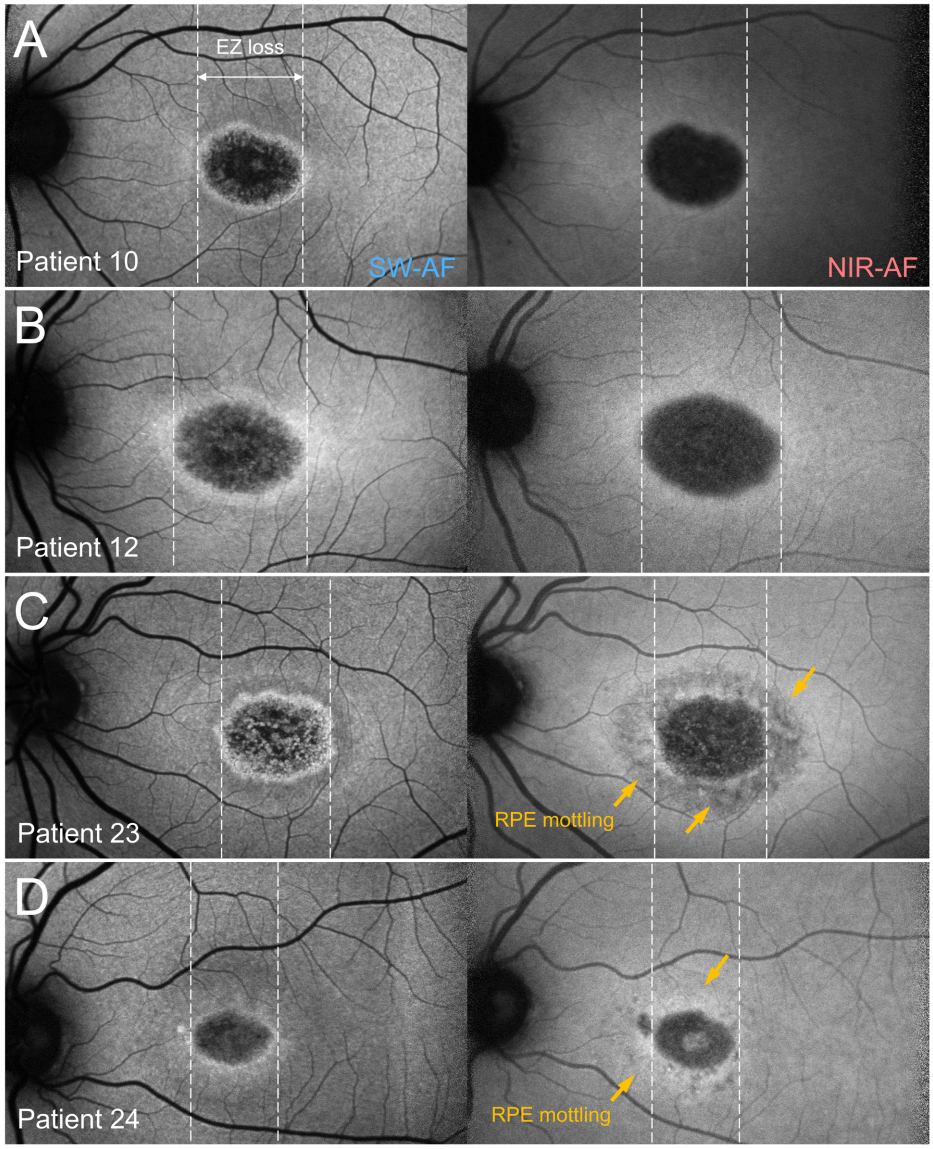


Figure 2: Short wavelength-autofluorescence (SW-AF) (left column) and near infrared-autofluorescence (NIR-AF) (right column) imaging of the atrophic lesion in the left eyes of (A) Patient 10, (B) Patient 12, (C) Patient 23 and (D) Patient 24. White, horizontal dotted lines mark the position of ellipsoid zone (EZ) loss within the atrophic lesion. Yellow arrows indicate perilesional RPE mottling on NIR-AF.

mm eccentricity, thickness in all except one (P18) returned to within $\pm 2\sigma$ of healthy eyes (Figure 4B). This region of significant TREC+ thinning (below $2\sigma$ ), referred to henceforth as the subclinical perilesional zone (SPZ), covers a mean distance of 1.18 mm ($\sigma$ = 0.48) and 1.25 mm ($\sigma$ = 0.36) on the temporal and nasal sides of the lesion border, respectively. There was no significant difference between the temporal and nasal SPZ widths (paired Wilcoxon signed rank test, P = 0.215964).

### 3.6 Genotype-phenotype correlations

The presence of hyper-reflective foci in the ONL was significantly lower amongst pure p.(Gly1961Glu) allele genotypes (8/15, 60%) compared to all other genotypes (11/12, 92%) (Fisher's exact test, two-tailed P = 0.0433). Similarly, the eyes with perilesional RPE mottling visible on NIR-AF were only observed in patients with other *ABCA4* genotypes (P1, P8 and P13) or complex/modified p.(Gly1961Glu) alleles (P19, P23 and P24) (Table 1). The precise region in the macula corresponding to this RPE mottling was not visibly evident on SD-OCT or thickness measurements. There

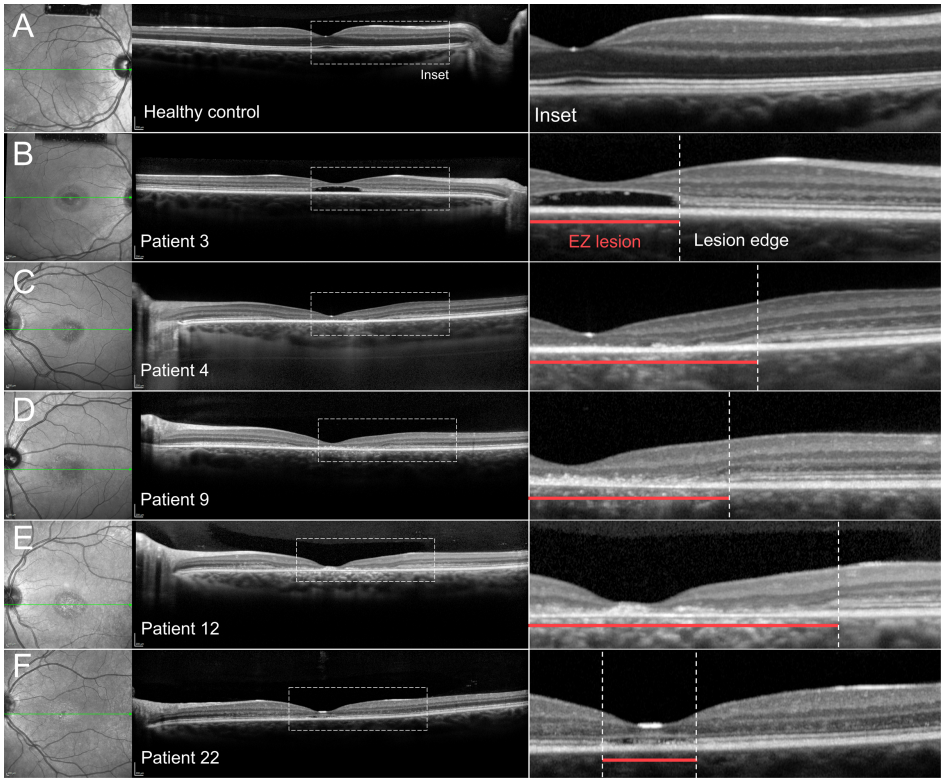


Figure 3: Horizontal spectral domain-optical coherence tomography (SD-OCT, 9mm) scans through the fovea in (A) a healthy control eye (N1), (B) Patient 3, (C) Patient 4, (D) Patient 9, (E) Patient 12 and (F) Patient 22. The corresponding position of each scan is indicated (green line) on infrared reflectance images of the macula. Red horizontal lines delineate the continuous area of EZ lesion and white vertical dotted lines mark the position of EZ disruption.

were no apparent differences in the extent of overall TREC+ thinning nor the mean size of the SPZ between pure p.(Gly1961Glu) allele genotypes and other *ABCA4* genotypes (MWU, P > 0.4) (Figure 4) (Table 2). This finding cannot be attributed to age differences, in fact, as patients with pure p.(Gly1961Glu) allele genotypes ($\mu_{age}$ = 26.7 years) were collectively older than patients with other *ABCA4* genotypes ($\mu_{age}$ = 20.8 years) at the time of examination.

## 4 Discussion

This study provides direct evidence for the existence of a subclinical perilesional zone, or SPZ, characterized by significant photoreceptor thinning disease around the perimeter of the atrophic lesion in patients with early stage ABCA4 disease. On horizontal SD-OCT scans, the average width of this SPZ is 1.21 mm ($\sigma$ = 0.379), or approximately 4.04°$\pm$ 1.26°. These parameters are consistent with the spatial mapping of visual function loss in several prior studies. Verdina et al. mapped the PRL of ABCA4 disease patients with remote fixation to 4.67°$\pm$ 2.38°from the edge of macular atrophy.[86] Similarly, Sunness et al. showed that in cases where the dense scotoma exceeds the size of the lesion, the excess length outside the lesion ranges from 3°- 4°(3 eyes), 5°- 6°(8 eyes) and $\geq$7°(6 eyes)..[80] The structural significance of photoreceptor thinning in ABCA4 disease is also well-documented and likely represents active cellular degeneration. Histopathological studies in canine ($ABCA4^{-/-}$)[19, 47] and mouse ($Abca4^{-/-}$, $Abca4^{PV/PV}$, $Abca4^{NS/NS}$)[51, 72, 97] models have attributed this thinning to the reduction in the number of photoreceptor nuclei. While there have been several *ex vivo* studies in human donor eyes, similar analyses of the photoreceptor layer have not been possible due to the advanced degeneration.[5, 18, 84] The observed absence of the IZ band in this study, a marker of degeneration in other degenerative disorders (CRD,[46] choroideremia[82] and acute zonal occult outer retinopathy[48]), outside the lesion in all patients may also be indicative of active degeneration in ABCA4 disease. It should be noted, however, that the IZ was indiscernible across the entire length of the SD-OCT scans (in all patients)–a finding that Park and colleagues have interpreted to be an artifact whereby the IZ band is visually obscured due to enhanced RPE reflectivity in ABCA4 disease patient eyes.[54] Elucidating the precise mechanistic details underlying

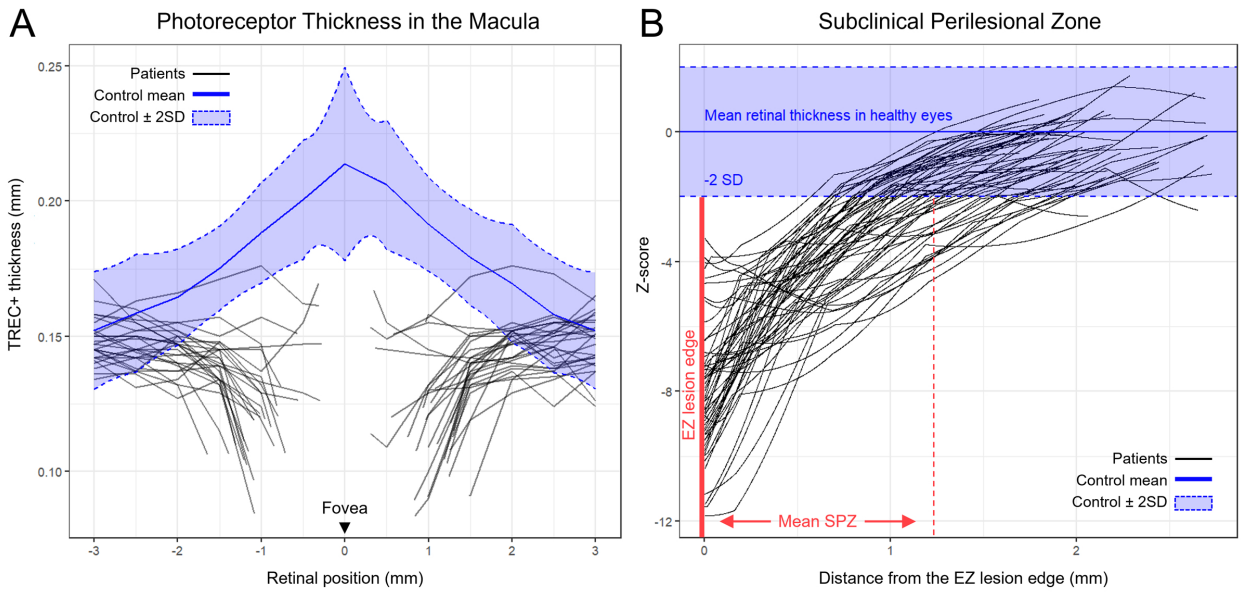


Figure 4: Quantification of perilesional photoreceptor layer thinning in spectral domain-optical coherence tomography (SD-OCT) scans in study eyes of patients with early stage ABCA4 disease. (A) Thickness profiles of total receptor+ (TREC) along SD-OCT in millimeters (mm) of 27 patient/eyes (black lines). Regions along the thickness profile spanning the atrophic lesion (ellipsoid zone (EZ) disruption) were removed for each patient/eye. Blue solid and dotted lines represent the mean ($\mu$ ) and $\pm$ 2 standard deviation ($\sigma$ ) boundaries, respectively, of the healthy control TREC+ thickness measured from 20 age-matched control eyes. Regions of thickness within the blue shaded area fall within normal limits ($\pm$ 2$\sigma$ ). All thickness profiles are represented as right eyes. The fovea is aligned at 0 along the x-axis; temporal positions are marked by negative values and nasal positions are marked by positive values. (B) Z-score profiles of TREC+ thinning from both as a function of distance (in mm) from the EZ lesion border. The vertical red dotted line marks the average distance of perilesional TREC+ thinning and average width of the subclinical perilesional zone (SPZ) in all study patients/eyes.

Table 2: Demographic, clinical and genetic characteristics of the study cohort.

| Patient | Age | Lesion radius | | Lesion diameter | SPZ width | | Mean SPZ width |
|---|---|---|---|---|---|---|---|
| | | Temporal | Nasal | | Temporal | Nasal | |
| All study eyes | | | | | | | |
| Mean | 24.1 | 0.907 | 0.927 | 1.726 | 1.175 | 1.25 | 1.212 |
| Median | 23.9 | 0.995 | 0.98 | 1.881 | 1.032 | 1.167 | 1.157 |
| SD | 12 | 0.351 | 0.333 | 0.701 | 0.476 | 0.358 | 0.379 |
| Other *ABCA4* | | | | | | | |
| Mean | 20.8 | 0.967 | 0.988 | 1.711 | 1.098 | 1.2 | 1.149 |
| Median | 19.6 | 1 | 0.984 | 1.825 | 0.878 | 1.164 | 1.158 |
| SD | 8.2 | 0.309 | 0.263 | 0.661 | 0.415 | 0.307 | 0.304 |
| p.(Gly1961Glu) | | | | | | | |
| Mean | 26.7 | 0.86 | 0.878 | 1.738 | 1.237 | 1.29 | 1.263 |
| Median | 24.2 | 0.957 | 0.936 | 1.926 | 1.103 | 1.38 | 1.157 |
| SD | 14.1 | 0.386 | 0.381 | 0.754 | 0.525 | 0.401 | 0.434 |
| Mann-Whitney U test | | | | | | | |
| P-value | 0.283 | 0.714 | 0.648 | 0.714 | 0.456 | 0.548 | 0.486 |
| Test statistic W | 112 | 82 | 80 | 82 | 106 | 103 | 105 |

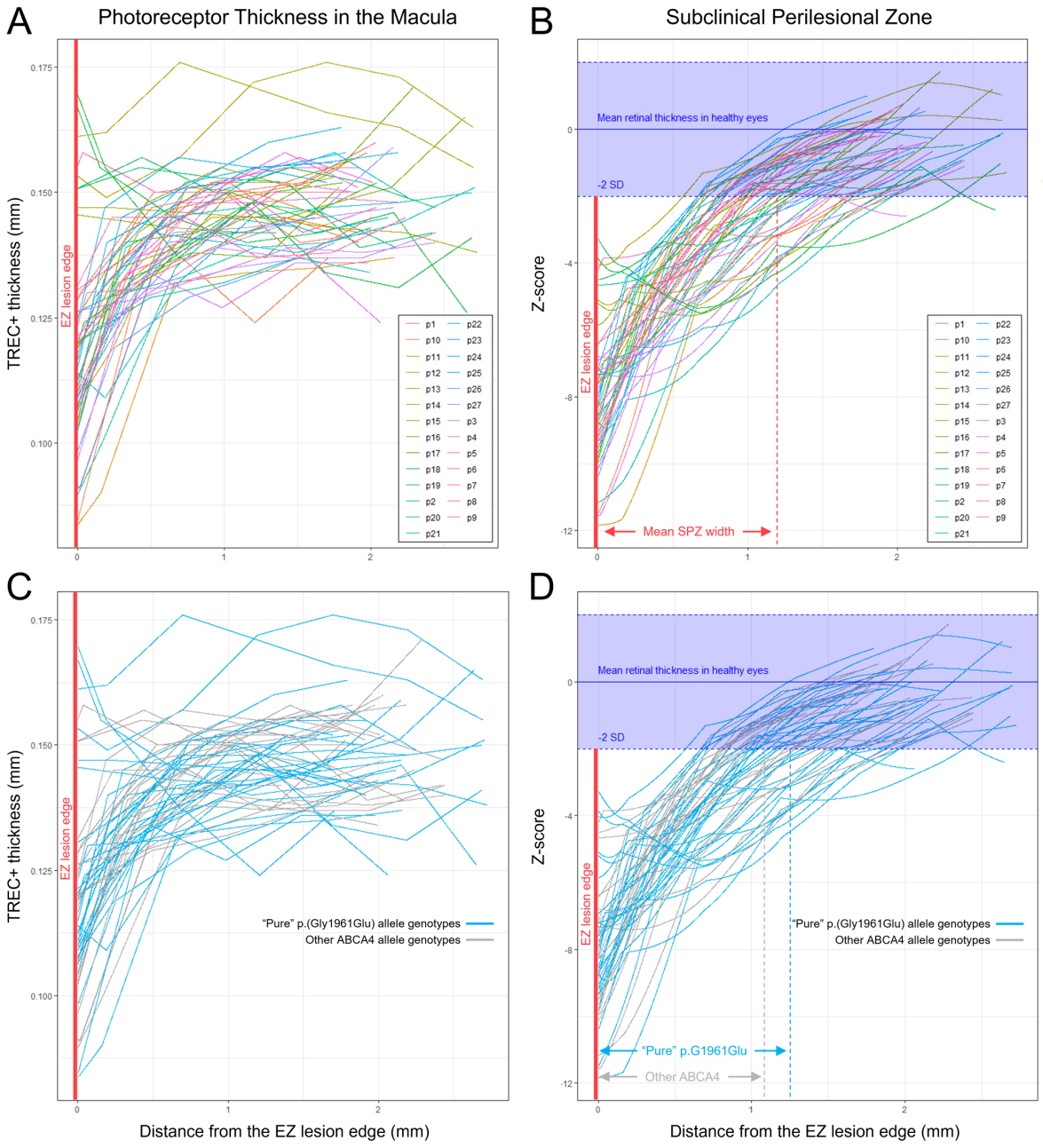


Figure 5: Quantification of perilesional photoreceptor layer thickness in spectral domain-optical coherence tomography (SD-OCT) scans in study eyes of individual patients and genotypes of early stage ABCA4 disease. (A) Temporal and nasal total receptor+ (TREC+) thickness profiles adjacent to the ellipsoid zone (EZ) lesion edge of individual patients/study eyes. (B) Z-score profiles of TREC+ thinning as a function of distance (in mm) from the EZ lesion border of individual patients/study eyes. Comparison of (C) TREC+ thickness and (D) Z-score profiles of perilesional zone thinning in p.(Gly1961Glu) genotypes (blue) and all other *ABCA4* genotypes (gray) patients/study eyes.

the SPZ is beyond the scope of this study, however, it is clear that considering these subclinical changes outside the visible lesion in the fundus is necessary to better approximate the total affected area of the macula in ABCA4 disease.

The recent emergence of potential therapies for ABCA4 disease has underscored the need for effective endpoint measures for clinical trials (`https://clinicaltrials.gov/search?cond=abca4`). This task is complicated in various ways due to the heterogeneous appearance of lesions (e.g., border delineation, atrophy subgrouping, etc.).[20] Currently, monitoring definitely decreased autofluorescence (DDAF) is the most commonly used method and serves as the primary outcome measure in several clinical trials: ALK-001 (NCT04239625), Emixustat (NCT03772665), Tinlarebant (NCT05244304), among others. While progression rates are well-documented and reproducible,[77, 76] the DDAF boundary does not represent the leading edge (both functional and structural) of disease progression compared to retinal layer thinning on OCT.[12, 78] Indeed, other non-invasive, higher resolution imaging modalities exist. Adaptive optics-scanning laser ophthalmoscopy (AO-SLO) resolves images of the retina at the cellular level[45, 90] and in fact, is capable of revealing subtle alterations including decreased cone density and increased spacing in areas of otherwise normal photoreceptor layer thickness.[15, 36, 68] Numerous technical hurdles specific to AO-SLO—the requirement of stable fixation, complexity of instrument operation, high costs and limited availability—limit its practical utility and makes OCT a more suitable endpoint modality for ABCA4 disease, at least in the near future.[7]

This study has several limitations. The SPZ was characterized using single horizontal SD-OCT scans which do not cover the entire area of the atrophic lesion. Additionally, the analysis was cross-sectional across a cohort, so individual progression rates could not be assessed. Further research with longitudinal volume scans, such as the recent large study by Pfau et al.,[57] is warranted. Our cohort size was also relatively small due to the study's design, which focused on thinning while minimizing confounding factors from secondary extra-lesional features like flecks. However, since these features are common in ABCA4 disease, future studies with larger cohorts that include patients with flecks are necessary to increase statistical rigor and broaden applicability to more patient subgroups. The strict inclusion criteria, which inherently selected for not only early-stage cases, but also milder variants like p.(Arg2107His),[96] p.(Val989Ala),[96] alongside p.(Gly1961Glu), may also explain the lack of observed genotype-phenotype correlations. Notably, no cases with biallelic null genotypes, which represent the most severe forms of ABCA4 disease,[13] were included. Expanding the inclusion criteria to incorporate such cases would not only require accounting for flecks, but also an increase in the imaging field beyond the 9 mm SD-OCT scans used here to capture larger, rapidly progressing lesions.

In conclusion, this study provides valuable insight into the subclinical perilesional zone (SPZ) in early-stage ABCA4 disease, highlighting the importance of photoreceptor thinning as a marker of active degeneration. While limitations such as cross-sectional analysis, a small cohort, and the exclusion of certain disease variants exist, our findings underscore the need for longitudinal studies with larger and more diverse patient groups. Future research should aim to further characterize the SPZ and refine imaging modalities, with the goal of improving endpoint measures for clinical trials and broadening their applicability to a wider range of ABCA4 disease cases.

## 5 Additional information

### 5.1 Funding

This work was supported, in part, by the National Eye Institute, NIH grants R01 EY028203, R01 EY028954, R01 EY029315, P30 19007 (Core Grant for Vision Research), the Foundation Fighting Blindness USA, grant no. PPA-1218-0751-COLU, and the unrestricted grant to the Department of Ophthalmology, Columbia University, from Research to Prevent Blindness.

### 5.2 Conflicts of interest

SHT has received support from Abeona Therapeutics and is a board member of Emendo Biotherapeutics, Nanoscope Therapeutics and Rejuvitas, Inc.

### 5.3 Author contributions

WL designed the study, recruited study participants, acquired and analyzed clinical and molecular data, supervised the study and wrote the manuscript; AZ helped design the study, analyzed de-identified data and critically revised the manuscript; PYS recruited participants and analyzed clinical data; JZ performed sequencing and analyzed molecular data; SHT clinically examined study participants; and RA supervised the study, critically revised the manuscript, and obtained research funding.

### 5.4 Data availability statement

All data produced in the present work are contained in the manuscript.

## References

[1] R. Allikmets et al. "A photoreceptor cell-specific ATP-binding transporter gene (ABCR) is mutated in recessive Stargardt macular dystrophy". In: *Nat Genet* 15.3 (1997), pp. 236–46. ISSN: 1061-4036 (Print) 1061-4036 (Linking). DOI: 10.1038/ng0397-236. URL: https://www.ncbi.nlm.nih.gov/pubmed/9054934.

[2] N. M. Bax et al. "The absence of fundus abnormalities in Stargardt disease". In: *Graefes Arch Clin Exp Ophthalmol* 257.6 (2019), pp. 1147–1157. ISSN: 1435-702X (Electronic) 0721-832X (Linking). DOI: 10.1007/s00417-019-04280-8. URL: https://www.ncbi.nlm.nih.gov/pubmed/30903310.

[3] S. Beharry, M. Zhong, and R. S. Molday. "N-retinylidene-phosphatidylethanolamine is the preferred retinoid substrate for the photoreceptor-specific ABC transporter ABCA4 (ABCR)". In: *J Biol Chem* 279.52 (2004), pp. 53972–9. ISSN: 0021-9258 (Print) 0021-9258 (Linking). DOI: 10.1074/jbc.M405216200. URL: https://www.ncbi.nlm.nih.gov/pubmed/15471866.

[4] A. Bernstein et al. "Mapping the Dense Scotoma and Its Enlargement in Stargardt Disease". In: *Retina* 36.9 (2016), pp. 1741–50. ISSN: 1539-2864 (Electronic) 0275-004X (Print) 0275-004X (Linking). DOI: 10.1097/IAE.0000000000001003. URL: https://www.ncbi.nlm.nih.gov/pubmed/26909568.

[5] V. L. Bonilha et al. "Retinal Histopathology in Eyes from a Patient with Stargardt disease caused by Compound Heterozygous ABCA4 Mutations". In: *Ophthalmic Genet* 37.2 (2016), pp. 150–60. ISSN: 1744-5094 (Electronic) 1381-6810 (Linking). DOI: 10.3109/13816810.2014.958861. URL: https://www.ncbi.nlm.nih.gov/pubmed/25265374.

[6] T. R. Burke et al. "Quantitative fundus autofluorescence in recessive Stargardt disease". In: *Invest Ophthalmol Vis Sci* 55.5 (2014), pp. 2841–52. ISSN: 1552-5783 (Electronic) 0146-0404 (Linking). DOI: 10.1167/iovs.13-13624. URL: https://www.ncbi.nlm.nih.gov/pubmed/24677105.

[7] J. Carroll et al. "Adaptive optics retinal imaging–clinical opportunities and challenges". In: *Curr Eye Res* 38.7 (2013), pp. 709–21. ISSN: 1460-2202 (Electronic) 0271-3683 (Print) 0271-3683 (Linking). DOI: 10.3109/02713683.2013.784792. URL: https://www.ncbi.nlm.nih.gov/pubmed/23621343.

[8] W. Cella et al. "G1961E mutant allele in the Stargardt disease gene ABCA4 causes bull's eye maculopathy". In: *Exp Eye Res* 89.1 (2009), pp. 16–24. ISSN: 1096-0007 (Electronic) 0014-4835 (Linking). DOI: 10.1016/j.exer.2009.02.001. URL: https://www.ncbi.nlm.nih.gov/pubmed/19217903.

[9] L. Ciccone et al. "Hyperreflective Deposition in the Background of Advanced Stargardt Disease". In: *Retina* 38.11 (2018), pp. 2214–2219. ISSN: 1539-2864 (Electronic) 0275-004X (Print) 0275-004X (Linking). DOI: 10.1097/IAE.0000000000001841. URL: https://www.ncbi.nlm.nih.gov/pubmed/29028687.

[10] A. V. Cideciyan et al. "Macular function in macular degenerations: repeatability of microperimetry as a potential outcome measure for ABCA4-associated retinopathy trials". In: *Invest Ophthalmol Vis Sci* 53.2 (2012), pp. 841–52. ISSN: 1552-5783 (Electronic) 0146-0404 (Linking). DOI: 10.1167/iovs.11-8415. URL: https://www.ncbi.nlm.nih.gov/pubmed/22247458.

[11] A. V. Cideciyan et al. "Mutations in ABCA4 result in accumulation of lipofuscin before slowing of the retinoid cycle: a reappraisal of the human disease sequence". In: *Hum Mol Genet* 13.5 (2004), pp. 525–34. ISSN: 0964-6906 (Print) 0964-6906 (Linking). DOI: 10.1093/hmg/ddh048. URL: https://www.ncbi.nlm.nih.gov/pubmed/14709597.

[12] A. V. Cideciyan et al. "Predicting Progression of ABCA4-Associated Retinal Degenerations Based on Longitudinal Measurements of the Leading Disease Front". In: *Invest Ophthalmol Vis Sci* 56.10 (2015), pp. 5946–55. ISSN: 1552-5783 (Electronic) 0146-0404 (Print) 0146-0404 (Linking). DOI: 10.1167/iovs.15-17698. URL: https://www.ncbi.nlm.nih.gov/pubmed/26377081.

[13] F. P. M. Cremers et al. "Clinical spectrum, genetic complexity and therapeutic approaches for retinal disease caused by ABCA4 mutations". In: *Prog Retin Eye Res* (2020), p. 100861. ISSN: 1873-1635 (Electronic) 1350-9462 (Linking). DOI: 10.1016/j.preteyeres.2020.100861. URL: https://www.ncbi.nlm.nih.gov/pubmed/32278709.

[14] C. A. Cukras et al. "Centrifugal expansion of fundus autofluorescence patterns in Stargardt disease over time". In: *Arch Ophthalmol* 130.2 (2012), pp. 171–9. ISSN: 1538-3601 (Electronic) 0003-9950 (Linking). DOI: 10.1001/archophthalmol.2011.332. URL: https://www.ncbi.nlm.nih.gov/pubmed/21987580.

[15] H. De Bruyn et al. "The Surviving, Not Thriving, Photoreceptors in Patients with ABCA4 Stargardt Disease". In: *Diagnostics (Basel)* 14.14 (2024). ISSN: 2075-4418 (Print) 2075-4418 (Electronic) 2075-4418 (Linking). DOI: 10.3390/diagnostics14141545. URL: https://www.ncbi.nlm.nih.gov/pubmed/39061682.

[16] A. F. Deutman. *The hereditary dystrophies of the posterior pole of the eye*. van Gorcum Comp. N.V., 1971.

[17] T. Duncker et al. "Correlations among near-infrared and short-wavelength autofluorescence and spectral-domain optical coherence tomography in recessive Stargardt disease". In: *Invest Ophthalmol Vis Sci* 55.12 (2014), pp. 8134–43. ISSN: 1552-5783 (Electronic) 0146-0404 (Linking). DOI: 10.1167/iovs.14-14848. URL: https://www.ncbi.nlm.nih.gov/pubmed/25342616.

[18] Jr. Eagle R. C. et al. "Retinal pigment epithelial abnormalities in fundus flavimaculatus: a light and electron microscopic study". In: *Ophthalmology* 87.12 (1980), pp. 1189–200. ISSN: 0161-6420 (Print) 0161-6420 (Linking). DOI: 10.1016/s0161-6420(80)35106-3. URL: https://www.ncbi.nlm.nih.gov/pubmed/6165950.

[19] B. Ekesten et al. "Abnormal Appearance of the Area Centralis in Labrador Retrievers With an ABCA4 Loss-of-function Mutation". In: *Transl Vis Sci Technol* 11.2 (2022), p. 36. ISSN: 2164-2591 (Electronic) 2164-2591 (Linking). DOI: 10.1167/tvst.11.2.36. URL: https://www.ncbi.nlm.nih.gov/pubmed/35201338.

[20] A. M. Ervin et al. "A Workshop on Measuring the Progression of Atrophy Secondary to Stargardt Disease in the ProgStar Studies: Findings and Lessons Learned". In: *Transl Vis Sci Technol* 8.2 (2019), p. 16. ISSN: 2164-2591 (Print) 2164-2591 (Electronic) 2164-2591 (Linking). DOI: 10.1167/tvst.8.2.16. URL: https://www.ncbi.nlm.nih.gov/pubmed/31019847.

[21] G. A. Fishman. "Fundus flavimaculatus. A clinical classification". In: *Arch Ophthalmol* 94.12 (1976), pp. 2061–7. ISSN: 0003-9950 (Print) 0003-9950 (Linking). DOI: 10.1001/archopht.1976.03910040721003. URL: https://www.ncbi.nlm.nih.gov/pubmed/999551.

[22] G. A. Fishman et al. "Variation of clinical expression in patients with Stargardt dystrophy and sequence variations in the ABCR gene". In: *Arch Ophthalmol* 117.4 (1999), pp. 504–10. ISSN: 0003-9950 (Print) 0003-9950 (Linking). DOI: 10.1001/archopht.117.4.504. URL: https://www.ncbi.nlm.nih.gov/pubmed/10206579.

[23] A. Franceschetti. "A special form of tapetoretinal degeneration: fundus flavimaculatus". In: *Trans Am Acad Ophthalmol Otolaryngol* 69.6 (1965), pp. 1048–53. ISSN: 0002-7154 (Print) 0002-7154 (Linking). URL: https://www.ncbi.nlm.nih.gov/pubmed/5861644.

[24] A. Franceschetti and J. François. "[Fundus flavimaculatus]". In: *Arch Ophtalmol Rev Gen Ophtalmol* 25.6 (1965), pp. 505–30. ISSN: 0003-973X (Print) 0003-973X (Linking). URL: https://www.ncbi.nlm.nih.gov/pubmed/4221555.

[25] J. Gersch et al. "Investigation of Structural Alterations in Inherited Retinal Diseases: A Quantitative SD-OCT-Analysis of Retinal Layer Thicknesses in Light of Underlying Genetic Mutations". In: *Int J Mol Sci* 23.24 (2022). ISSN: 1422-0067 (Electronic) 1422-0067 (Linking). DOI: 10.3390/ijms232416007. URL: https://www.ncbi.nlm.nih.gov/pubmed/36555650.

[26] V. C. Greenstein et al. "A Comparison of En Face Optical Coherence Tomography and Fundus Autofluorescence in Stargardt Disease". In: *Invest Ophthalmol Vis Sci* 58.12 (2017), pp. 5227–5236. ISSN: 1552-5783 (Electronic) 0146-0404 (Print) 0146-0404 (Linking). DOI: 10.1167/iovs.17-22532. URL: https://www.ncbi.nlm.nih.gov/pubmed/29049723.

[27] V. C. Greenstein et al. "Preferred retinal locus in macular disease: characteristics and clinical implications". In: *Retina* 28.9 (2008), pp. 1234–40. ISSN: 1539-2864 (Electronic) 0275-004X (Print) 0275-004X (Linking). DOI: 10.1097/IAE.0b013e31817c1b47. URL: https://www.ncbi.nlm.nih.gov/pubmed/18628727.

[28] D. C. Hood et al. "Thickness of receptor and post-receptor retinal layers in patients with retinitis pigmentosa measured with frequency-domain optical coherence tomography". In: *Invest Ophthalmol Vis Sci* 50.5 (2009), pp. 2328–36. ISSN: 1552-5783 (Electronic) 0146-0404 (Print) 0146-0404 (Linking). DOI: 10.1167/iovs.08-2936. URL: https://www.ncbi.nlm.nih.gov/pubmed/19011017.

[29] D. Huang et al. "Optical coherence tomography". In: *Science* 254.5035 (1991), pp. 1178–81. ISSN: 0036-8075 (Print) 1095-9203 (Electronic) 0036-8075 (Linking). DOI: 10.1126/science.1957169. URL: https://www.ncbi.nlm.nih.gov/pubmed/1957169.

[30] N. M. Ioannidis et al. "REVEL: An Ensemble Method for Predicting the Pathogenicity of Rare Missense Variants". In: *Am J Hum Genet* 99.4 (2016), pp. 877–885. ISSN: 1537-6605 (Electronic) 0002-9297 (Print) 0002-9297 (Linking). DOI: 10.1016/j.ajhg.2016.08.016. URL: https://www.ncbi.nlm.nih.gov/pubmed/27666373.

[31] I. Ionita-Laza et al. "A spectral approach integrating functional genomic annotations for coding and noncoding variants". In: *Nat Genet* 48.2 (2016), pp. 214–20. ISSN: 1546-1718 (Electronic) 1061-4036 (Linking). DOI: 10.1038/ng.3477. URL: https://www.ncbi.nlm.nih.gov/pubmed/26727659.

[32] K. A. Jagadeesh et al. "M-CAP eliminates a majority of variants of uncertain significance in clinical exomes at high sensitivity". In: *Nat Genet* 48.12 (2016), pp. 1581–1586. ISSN: 1546-1718 (Electronic) 1061-4036 (Linking). DOI: 10.1038/ng.3703. URL: https://www.ncbi.nlm.nih.gov/pubmed/27776117.

[33] K. Jaganathan et al. "Predicting Splicing from Primary Sequence with Deep Learning". In: *Cell* 176.3 (2019), 535–548 e24. ISSN: 1097-4172 (Electronic) 0092-8674 (Linking). DOI: 10.1016/j.cell.2018.12.015. URL: https://www.ncbi.nlm.nih.gov/pubmed/30661751.

[34] R. S. Jonnal et al. "The cellular origins of the outer retinal bands in optical coherence tomography images". In: *Invest Ophthalmol Vis Sci* 55.12 (2014), pp. 7904–18. ISSN: 1552-5783 (Electronic) 0146-0404 (Print) 0146-0404 (Linking). DOI: 10.1167/iovs.14-14907. URL: https://www.ncbi.nlm.nih.gov/pubmed/25324288.

[35] S. Kellner et al. "Lipofuscin- and melanin-related fundus autofluorescence in patients with ABCA4-associated retinal dystrophies". In: *Am J Ophthalmol* 147.5 (2009), 895–902, 902 e1. ISSN: 1879-1891 (Electronic) 0002-9394 (Linking). DOI: 10.1016/j.ajo.2008.12.023. URL: https://www.ncbi.nlm.nih.gov/pubmed/19243736.

[36] K. N. Khan et al. "Early Patterns of Macular Degeneration in ABCA4-Associated Retinopathy". In: *Ophthalmology* 125.5 (2018), pp. 735–746. ISSN: 1549-4713 (Electronic) 0161-6420 (Linking). DOI: 10.1016/j.ophtha.2017.11.020. URL: https://www.ncbi.nlm.nih.gov/pubmed/29310964.

[37] M. Kircher et al. "A general framework for estimating the relative pathogenicity of human genetic variants". In: *Nat Genet* 46.3 (2014), pp. 310–5. ISSN: 1546-1718 (Electronic) 1061-4036 (Print) 1061-4036 (Linking). DOI: 10.1038/ng.2892. URL: https://www.ncbi.nlm.nih.gov/pubmed/24487276.

[38] X. Kong et al. "Reproducibility of Measurements of Retinal Structural Parameters Using Optical Coherence Tomography in Stargardt Disease". In: *Transl Vis Sci Technol* 8.3 (2019), p. 46. ISSN: 2164-2591 (Print) 2164-2591 (Electronic) 2164-2591 (Linking). DOI: 10.1167/tvst.8.3.46. URL: https://www.ncbi.nlm.nih.gov/pubmed/31259091.

[39] U. Kretschmann et al. "Multifocal electroretinography in patients with Stargardt's macular dystrophy". In: *Br J Ophthalmol* 82.3 (1998), pp. 267–75. ISSN: 0007-1161 (Print) 1468-2079 (Electronic) 0007-1161 (Linking). DOI: 10.1136/bjo.82.3.267. URL: https://www.ncbi.nlm.nih.gov/pubmed/9602623.

[40] K. Kuniyoshi et al. "Multifocal electroretinograms in Stargardt's disease/fundus flavimaculatus". In: *Ophthalmologica* 232.2 (2014), pp. 118–25. ISSN: 1423-0267 (Electronic) 0030-3755 (Linking). DOI: 10.1159/000361056. URL: https://www.ncbi.nlm.nih.gov/pubmed/24970593.

[41] M. A. Lazow et al. "Transition zones between healthy and diseased retina in choroideremia (CHM) and Stargardt disease (STGD) as compared to retinitis pigmentosa (RP)". In: *Invest Ophthalmol Vis Sci* 52.13 (2011), pp. 9581–90. ISSN: 1552-5783 (Electronic) 0146-0404 (Print) 0146-0404 (Linking). DOI: 10.1167/iovs.11-8554. URL: https://www.ncbi.nlm.nih.gov/pubmed/22076985.

[42] W. Lee et al. "A genotype-phenotype correlation matrix for ABCA4 disease based on long-term prognostic outcomes". In: *JCI Insight* 7.2 (2022). ISSN: 2379-3708 (Electronic) 2379-3708 (Linking). DOI: 10.1172/jci.insight.156154. URL: https://www.ncbi.nlm.nih.gov/pubmed/34874912.

[43] W. Lee et al. "Cis-acting modifiers in the ABCA4 locus contribute to the penetrance of the major disease-causing variant in Stargardt disease". In: *Hum Mol Genet* 30.14 (2021), pp. 1293–1304. ISSN: 1460-2083 (Electronic) 0964-6906 (Print) 0964-6906 (Linking). DOI: 10.1093/hmg/ddab122. URL: https://www.ncbi.nlm.nih.gov/pubmed/33909047.

[44] W. Lee et al. "The external limiting membrane in early-onset Stargardt disease". In: *Invest Ophthalmol Vis Sci* 55.10 (2014), pp. 6139–49. ISSN: 1552-5783 (Electronic) 0146-0404 (Linking). DOI: 10.1167/iovs.14-15126. URL: https://www.ncbi.nlm.nih.gov/pubmed/25139735.

[45] J. Liang, D. R. Williams, and D. T. Miller. "Supernormal vision and high-resolution retinal imaging through adaptive optics". In: *J Opt Soc Am A Opt Image Sci Vis* 14.11 (1997), pp. 2884–92. ISSN: 1084-7529 (Print) 1084-7529 (Linking). DOI: 10.1364/josaa.14.002884. URL: https://www.ncbi.nlm.nih.gov/pubmed/9379246.

[46] L. H. Lima, J. M. Sallum, and R. F. Spaide. "Outer retina analysis by optical coherence tomography in cone-rod dystrophy patients". In: *Retina* 33.9 (2013), pp. 1877–80. ISSN: 1539-2864 (Electronic) 0275-004X (Linking). DOI: 10.1097/IAE.0b013e31829234e6. URL: https://www.ncbi.nlm.nih.gov/pubmed/23648999.

[47] S. Makelainen et al. "An ABCA4 loss-of-function mutation causes a canine form of Stargardt disease". In: *PLoS Genet* 15.3 (2019), e1007873. ISSN: 1553-7404 (Electronic) 1553-7390 (Print) 1553-7390 (Linking). DOI: 10.1371/journal.pgen.1007873. URL: https://www.ncbi.nlm.nih.gov/pubmed/30889179.

[48] Y. Matsui et al. "Changes in outer retinal microstructures during six month period in eyes with acute zonal occult outer retinopathy-complex". In: *PLoS One* 9.10 (2014), e110592. ISSN: 1932-6203 (Electronic) 1932-6203 (Linking). DOI: 10.1371/journal.pone.0110592. URL: https://www.ncbi.nlm.nih.gov/pubmed/25356549.

[49] A. Maugeri et al. "Mutations in the ABCA4 (ABCR) gene are the major cause of autosomal recessive cone-rod dystrophy". In: *Am J Hum Genet* 67.4 (2000), pp. 960–6. ISSN: 0002-9297 (Print) 0002-9297 (Linking). DOI: 10.1086/303079. URL: https://www.ncbi.nlm.nih.gov/pubmed/10958761.

[50] P. Melillo et al. "En Face Spectral-Domain Optical Coherence Tomography for the Monitoring of Lesion Area Progression in Stargardt Disease". In: *Invest Ophthalmol Vis Sci* 57.9 (2016), OCT247–52. ISSN: 1552-5783 (Electronic) 0146-0404 (Print) 0146-0404 (Linking). DOI: 10.1167/iovs.15-18751. URL: https://www.ncbi.nlm.nih.gov/pubmed/27409479.

[51] L. L. Molday et al. "Localization and functional characterization of the p.Asn965Ser (N965S) ABCA4 variant in mice reveal pathogenic mechanisms underlying Stargardt macular degeneration". In: *Hum Mol Genet* 27.2 (2018), pp. 295–306. ISSN: 1460-2083 (Electronic) 0964-6906 (Print) 0964-6906 (Linking). DOI: 10.1093/hmg/ddx400. URL: https://www.ncbi.nlm.nih.gov/pubmed/29145636.

[52] D. P. Mucciolo et al. "Outer nuclear layer relevance in visual function correlated to quantitative enface OCT parameters in Stargardt disease". In: *Eur J Ophthalmol* 31.6 (2021), pp. 3248–3258. ISSN: 1724-6016 (Electronic) 1120-6721 (Linking). DOI: 10.1177/1120672121990579. URL: https://www.ncbi.nlm.nih.gov/pubmed/33508977.

[53] P. L. Muller et al. "Functional Relevance and Structural Correlates of Near Infrared and Short Wavelength Fundus Autofluorescence Imaging in ABCA4-Related Retinopathy". In: *Transl Vis Sci Technol* 8.6 (2019), p. 46. ISSN: 2164-2591 (Print) 2164-2591 (Electronic) 2164-2591 (Linking). DOI: 10.1167/tvst.8.6.46. URL: https://www.ncbi.nlm.nih.gov/pubmed/31879568.

[54] J. C. Park et al. "Objective Analysis of Hyperreflective Outer Retinal Bands Imaged by Optical Coherence Tomography in Patients With Stargardt Disease". In: *Invest Ophthalmol Vis Sci* 56.8 (2015), pp. 4662–7. ISSN: 1552-5783 (Electronic) 0146-0404 (Print) 0146-0404 (Linking). DOI: 10.1167/iovs.15-16955. URL: https://www.ncbi.nlm.nih.gov/pubmed/26207301.

[55] R. Parmann et al. "Comparisons Among Optical Coherence Tomography and Fundus Autofluorescence Modalities as Measurements of Atrophy in ABCA4-Associated Disease". In: *Transl Vis Sci Technol* 11.1 (2022), p. 36. ISSN: 2164-2591 (Electronic) 2164-2591 (Linking). DOI: 10.1167/tvst.11.1.36. URL: https://www.ncbi.nlm.nih.gov/pubmed/35089312.

[56] M. Pfau et al. "Light Sensitivity Within Areas of Geographic Atrophy Secondary to Age-Related Macular Degeneration". In: *Invest Ophthalmol Vis Sci* 60.12 (2019), pp. 3992–4001. ISSN: 1552-5783 (Electronic) 0146-0404 (Linking). DOI: 10.1167/iovs.19-27178. URL: https://www.ncbi.nlm.nih.gov/pubmed/31560765.

[57] M. Pfau et al. "Photoreceptor degeneration in ABCA4-associated retinopathy and its genetic correlates". In: *JCI Insight* 7.2 (2022). ISSN: 2379-3708 (Electronic) 2379-3708 (Linking). DOI: 10.1172/jci.insight.155373. URL: https://www.ncbi.nlm.nih.gov/pubmed/35076026.

[58] K. S. Pollard et al. "Detection of nonneutral substitution rates on mammalian phylogenies". In: *Genome Res* 20.1 (2010), pp. 110–21. ISSN: 1549-5469 (Electronic) 1088-9051 (Print) 1088-9051 (Linking). DOI: 10.1101/gr.097857.109. URL: https://www.ncbi.nlm.nih.gov/pubmed/19858363.

[59] J. Reinhard et al. "Quantifying fixation in patients with Stargardt disease". In: *Vision Res* 47.15 (2007), pp. 2076–85. ISSN: 0042-6989 (Print) 0042-6989 (Linking). DOI: 10.1016/j.visres.2007.04.012. URL: https://www.ncbi.nlm.nih.gov/pubmed/17562343.

[60] P. Rentzsch et al. "CADD: predicting the deleteriousness of variants throughout the human genome". In: *Nucleic Acids Res* 47.D1 (2019), pp. D886–D894. ISSN: 1362-4962 (Electronic) 0305-1048 (Print) 0305-1048 (Linking). DOI: 10.1093/nar/gky1016. URL: https://www.ncbi.nlm.nih.gov/pubmed/30371827.

[61] E. H. Runhart et al. "Late-Onset Stargardt Disease Due to Mild, Deep-Intronic ABCA4 Alleles". In: *Invest Ophthalmol Vis Sci* 60.13 (2019), pp. 4249–4256. ISSN: 1552-5783 (Electronic) 0146-0404 (Linking). DOI: 10.1167/iovs.19-27524. URL: https://www.ncbi.nlm.nih.gov/pubmed/31618761.

[62] E. H. Runhart et al. "The Common ABCA4 Variant p.Asn1868Ile Shows Nonpenetrance and Variable Expression of Stargardt Disease When Present in trans With Severe Variants". In: *Invest Ophthalmol Vis Sci* 59.8 (2018), pp. 3220–3231. ISSN: 1552-5783 (Electronic) 0146-0404 (Linking). DOI: 10.1167/iovs.18-23881. URL: https://www.ncbi.nlm.nih.gov/pubmed/29971439.

[63] R. Sangermano et al. "Deep-intronic ABCA4 variants explain missing heritability in Stargardt disease and allow correction of splice defects by antisense oligonucleotides". In: *Genet Med* 21.8 (2019), pp. 1751–1760. ISSN: 1530-0366 (Electronic) 1098-3600 (Linking). DOI: 10.1038/s41436-018-0414-9. URL: https://www.ncbi.nlm.nih.gov/pubmed/30643219.

[64] E. M. Schonbach et al. "Fixation Location and Stability Using the MP-1 Microperimeter in Stargardt Disease: ProgStar Report No. 3". In: *Ophthalmol Retina* 1.1 (2017), pp. 68–76. ISSN: 2468-6530 (Electronic) 2468-6530 (Linking). DOI: 10.1016/j.oret.2016.08.009. URL: https://www.ncbi.nlm.nih.gov/pubmed/31047397.

[65] E. M. Schonbach et al. "Longitudinal Changes of Fixation Location and Stability Within 12 Months in Stargardt Disease: ProgStar Report No. 12". In: *Am J Ophthalmol* 193 (2018), pp. 54–61. ISSN: 1879-1891 (Electronic) 0002-9394 (Print) 0002-9394 (Linking). DOI: 10.1016/j.ajo.2018.06.003. URL: https://www.ncbi.nlm.nih.gov/pubmed/29890160.

[66] R. A. Sisk and T. Leng. "Multimodal imaging and multifocal electroretinography demonstrate autosomal recessive Stargardt disease may present like occult macular dystrophy". In: *Retina* 34.8 (2014), pp. 1567–75. ISSN: 1539-2864 (Electronic) 0275-004X (Linking). DOI: 10.1097/IAE.0000000000000136. URL: https://www.ncbi.nlm.nih.gov/pubmed/24743636.

[67] A. Sodi et al. "En face OCT in Stargardt disease". In: *Graefes Arch Clin Exp Ophthalmol* 254.9 (2016), pp. 1669–79. ISSN: 1435-702X (Electronic) 0721-832X (Linking). DOI: 10.1007/s00417-015-3254-1. URL: https://www.ncbi.nlm.nih.gov/pubmed/26743751.

[68] H. Song et al. "Cone and rod loss in Stargardt disease revealed by adaptive optics scanning light ophthalmoscopy". In: *JAMA Ophthalmol* 133.10 (2015), pp. 1198–203. ISSN: 2168-6173 (Electronic) 2168-6165 (Print) 2168-6165 (Linking). DOI: 10.1001/jamaophthalmol.2015.2443. URL: https://www.ncbi.nlm.nih.gov/pubmed/26247787.

[69] J. R. Sparrow, K. Nakanishi, and C. A. Parish. "The lipofuscin fluorophore A2E mediates blue light-induced damage to retinal pigmented epithelial cells". In: *Invest Ophthalmol Vis Sci* 41.7 (2000), pp. 1981–9. ISSN: 0146-0404 (Print) 0146-0404 (Linking). URL: https://www.ncbi.nlm.nih.gov/pubmed/10845625.

[70] J. R. Sparrow et al. "A2E, a lipofuscin fluorophore, in human retinal pigmented epithelial cells in culture". In: *Invest Ophthalmol Vis Sci* 40.12 (1999), pp. 2988–95. ISSN: 0146-0404 (Print) 0146-0404 (Linking). URL: https://www.ncbi.nlm.nih.gov/pubmed/10549662.

[71] J. R. Sparrow et al. "Flecks in Recessive Stargardt Disease: Short-Wavelength Autofluorescence, Near-Infrared Autofluorescence, and Optical Coherence Tomography". In: *Invest Ophthalmol Vis Sci* 56.8 (2015), pp. 5029–39. ISSN: 1552-5783 (Electronic) 0146-0404 (Linking). DOI: 10.1167/iovs.15-16763. URL: https://www.ncbi.nlm.nih.gov/pubmed/26230768.

[72] J. R. Sparrow et al. "Quantitative fundus autofluorescence in mice: correlation with HPLC quantitation of RPE lipofuscin and measurement of retina outer nuclear layer thickness". In: *Invest Ophthalmol Vis Sci* 54.4 (2013), pp. 2812–20. ISSN: 1552-5783 (Electronic) 0146-0404 (Print) 0146-0404 (Linking). DOI: 10.1167/iovs.12-11490. URL: https://www.ncbi.nlm.nih.gov/pubmed/23548623.

[73] J. R. Sparrow et al. "The bisretinoids of retinal pigment epithelium". In: *Prog Retin Eye Res* 31.2 (2012), pp. 121–35. ISSN: 1873-1635 (Electronic) 1350-9462 (Linking). DOI: 10.1016/j.preteyeres.2011.12.001. URL: https://www.ncbi.nlm.nih.gov/pubmed/22209824.

[74] K Stargardt. "Über familiäre, progressive degeneration in der maculagegend des auges". In: *Albrecht von Graefes Arch Klin Ophthalmology* 71 (1909), pp. 534–550.

[75] R. W. Strauss et al. "Incidence of Atrophic Lesions in Stargardt Disease in the Progression of Atrophy Secondary to Stargardt Disease (ProgStar) Study: Report No. 5". In: *JAMA Ophthalmol* 135.7 (2017), pp. 687–695. ISSN: 2168-6173 (Electronic) 2168-6165 (Linking). DOI: 10.1001/jamaophthalmol.2017.1121. URL: https://www.ncbi.nlm.nih.gov/pubmed/28542697.

[76] R. W. Strauss et al. "Progression of Stargardt Disease as Determined by Fundus Autofluorescence in the Retrospective Progression of Stargardt Disease Study (ProgStar Report No. 9)". In: *JAMA Ophthalmol* 135.11 (2017), pp. 1232–1241. ISSN: 2168-6173 (Electronic) 2168-6165 (Print) 2168-6165 (Linking). DOI: 10.1001/jamaophthalmol.2017.4152. URL: https://www.ncbi.nlm.nih.gov/pubmed/29049437.

[77] R. W. Strauss et al. "Progression of Stargardt Disease as Determined by Fundus Autofluorescence Over a 24-Month Period (ProgStar Report No. 17)". In: *Am J Ophthalmol* 250 (2023), pp. 157–170. ISSN: 1879-1891 (Electronic) 0002-9394 (Linking). DOI: 10.1016/j.ajo.2023.02.003. URL: https://www.ncbi.nlm.nih.gov/pubmed/36764427.

[78] R. W. Strauss et al. "The Progression of Stargardt Disease as Determined by Spectral-Domain Optical Coherence Tomography over a 24-Month Period (ProgStar Report No. 18)". In: *Ophthalmic Res* 67.1 (2024), pp. 435–447. ISSN: 1423-0259 (Electronic) 0030-3747 (Linking). DOI: 10.1159/000540028. URL: https://www.ncbi.nlm.nih.gov/pubmed/39004077.

[79] J. S. Sunness and J. N. Steiner. "Retinal function and loss of autofluorescence in stargardt disease". In: *Retina* 28.6 (2008), pp. 794–800. ISSN: 0275-004X (Print) 0275-004X (Linking). DOI: 10.1097/IAE.0b013e31816690bd. URL: https://www.ncbi.nlm.nih.gov/pubmed/18536594.

[80] J. S. Sunness et al. "Abnormal Visual Function Outside the Area of Atrophy Defined by Short-Wavelength Fundus Autofluorescence in Stargardt Disease". In: *Invest Ophthalmol Vis Sci* 61.4 (2020), p. 36. ISSN: 1552-5783 (Electronic) 0146-0404 (Print) 0146-0404 (Linking). DOI: 10.1167/iovs.61.4.36. URL: https://www.ncbi.nlm.nih.gov/pubmed/32334431.

[81] J. S. Sunness et al. "Fixation patterns and reading rates in eyes with central scotomas from advanced atrophic age-related macular degeneration and Stargardt disease". In: *Ophthalmology* 103.9 (1996), pp. 1458–66. ISSN: 0161-6420 (Print) 1549-4713 (Electronic) 0161-6420 (Linking). DOI: 10.1016/s0161-6420(96)30483-1. URL: https://www.ncbi.nlm.nih.gov/pubmed/8841306.

[82] R. Syed et al. "High-resolution images of retinal structure in patients with choroideremia". In: *Invest Ophthalmol Vis Sci* 54.2 (2013), pp. 950–61. ISSN: 1552-5783 (Electronic) 0146-0404 (Print) 0146-0404 (Linking). DOI: 10.1167/iovs.12-10707. URL: https://www.ncbi.nlm.nih.gov/pubmed/23299470.

[83] K. Tanaka et al. "The Rapid-Onset Chorioretinopathy Phenotype of ABCA4 Disease". In: *Ophthalmology* 125.1 (2018), pp. 89–99. ISSN: 1549-4713 (Electronic) 0161-6420 (Linking). DOI: 10.1016/j.ophtha.2017.07.019. URL: https://www.ncbi.nlm.nih.gov/pubmed/28947085.

[84] T. Taubitz et al. "Ultrastructural alterations in the retinal pigment epithelium and photoreceptors of a Stargardt patient and three Stargardt mouse models: indication for the central role of RPE melanin in oxidative stress". In: *PeerJ* 6 (2018), e5215. ISSN: 2167-8359 (Print) 2167-8359 (Electronic) 2167-8359 (Linking). DOI: 10.7717/peerj.5215. URL: https://www.ncbi.nlm.nih.gov/pubmed/30038866.

[85] T. Vandenbroucke et al. "Colour Vision in Stargardt Disease". In: *Ophthalmic Res* 54.4 (2015), pp. 181–94. ISSN: 1423-0259 (Electronic) 0030-3747 (Linking). DOI: 10.1159/000438906. URL: https://www.ncbi.nlm.nih.gov/pubmed/26492201.

[86] T. Verdina et al. "Multimodal analysis of the Preferred Retinal Location and the Transition Zone in patients with Stargardt Disease". In: *Graefes Arch Clin Exp Ophthalmol* 255.7 (2017), pp. 1307–1317. ISSN: 1435-702X (Electronic) 0721-832X (Print) 0721-832X (Linking). DOI: 10.1007/s00417-017-3637-6. URL: https://www.ncbi.nlm.nih.gov/pubmed/28365912.

[87] K. Wang, M. Li, and H. Hakonarson. "ANNOVAR: functional annotation of genetic variants from high-throughput sequencing data". In: *Nucleic Acids Res* 38.16 (2010), e164. ISSN: 1362-4962 (Electronic) 0305-1048 (Linking). DOI: 10.1093/nar/gkq603. URL: https://www.ncbi.nlm.nih.gov/pubmed/20601685.

[88] Y. Wang et al. "The central retinal thickness and its related genotype in ABCA4-related retinopathy". In: *Eye (Lond)* (2024). ISSN: 1476-5454 (Electronic) 0950-222X (Linking). DOI: 10.1038/s41433-024-03104-2. URL: https://www.ncbi.nlm.nih.gov/pubmed/38740961.

[89] S. S. Whitmore et al. "Analysis of retinal sublayer thicknesses and rates of change in ABCA4-associated Stargardt disease". In: *Sci Rep* 10.1 (2020), p. 16576. ISSN: 2045-2322 (Electronic) 2045-2322 (Linking). DOI: 10.1038/s41598-020-73645-5. URL: https://www.ncbi.nlm.nih.gov/pubmed/33024232.

[90] D. R. Williams et al. "Evolution of adaptive optics retinal imaging [Invited]". In: *Biomed Opt Express* 14.3 (2023), pp. 1307–1338. ISSN: 2156-7085 (Print) 2156-7085 (Electronic) 2156-7085 (Linking). DOI: 10.1364/BOE.485371. URL: https://www.ncbi.nlm.nih.gov/pubmed/36950228.

[91] T. Zeng and Y. I. Li. "Predicting RNA splicing from DNA sequence using Pangolin". In: *Genome Biol* 23.1 (2022), p. 103. ISSN: 1474-760X (Electronic) 1474-7596 (Print) 1474-7596 (Linking). DOI: 10.1186/s13059-022-02664-4. URL: https://www.ncbi.nlm.nih.gov/pubmed/35449021.

[92] J. Zernant et al. "Analysis of the ABCA4 gene by next-generation sequencing". In: *Invest Ophthalmol Vis Sci* 52.11 (2011), pp. 8479–87. ISSN: 1552-5783 (Electronic) 0146-0404 (Linking). DOI: 10.1167/iovs.11-8182. URL: https://www.ncbi.nlm.nih.gov/pubmed/21911583.

[93] J. Zernant et al. "Analysis of the ABCA4 genomic locus in Stargardt disease". In: *Hum Mol Genet* 23.25 (2014), pp. 6797–806. ISSN: 1460-2083 (Electronic) 0964-6906 (Linking). DOI: 10.1093/hmg/ddu396. URL: https://www.ncbi.nlm.nih.gov/pubmed/25082829.

[94] J. Zernant et al. "Extremely hypomorphic and severe deep intronic variants in the ABCA4 locus result in varying Stargardt disease phenotypes". In: *Cold Spring Harb Mol Case Stud* 4.4 (2018). ISSN: 2373-2873 (Electronic) 2373-2873 (Linking). DOI: 10.1101/mcs.a002733. URL: https://www.ncbi.nlm.nih.gov/pubmed/29848554.

[95] J. Zernant et al. "Frequent hypomorphic alleles account for a significant fraction of ABCA4 disease and distinguish it from age-related macular degeneration". In: *J Med Genet* 54.6 (2017), pp. 404–412. ISSN: 1468-6244 (Electronic) 0022-2593 (Linking). DOI: 10.1136/jmedgenet-2017-104540. URL: https://www.ncbi.nlm.nih.gov/pubmed/28446513.

[96] J. Zernant et al. "Genetic and clinical analysis of ABCA4-associated disease in African American patients". In: *Hum Mutat* 35.10 (2014), pp. 1187–94. ISSN: 1098-1004 (Electronic) 1059-7794 (Print) 1059-7794 (Linking). DOI: 10.1002/humu.22626. URL: https://www.ncbi.nlm.nih.gov/pubmed/25066811.

[97] N. Zhang et al. "Protein misfolding and the pathogenesis of ABCA4-associated retinal degenerations". In: *Hum Mol Genet* 24.11 (2015), pp. 3220–37. ISSN: 1460-2083 (Electronic) 0964-6906 (Print) 0964-6906 (Linking). DOI: 10.1093/hmg/ddv073. URL: https://www.ncbi.nlm.nih.gov/pubmed/25712131.

## 6 Supplemental Materials

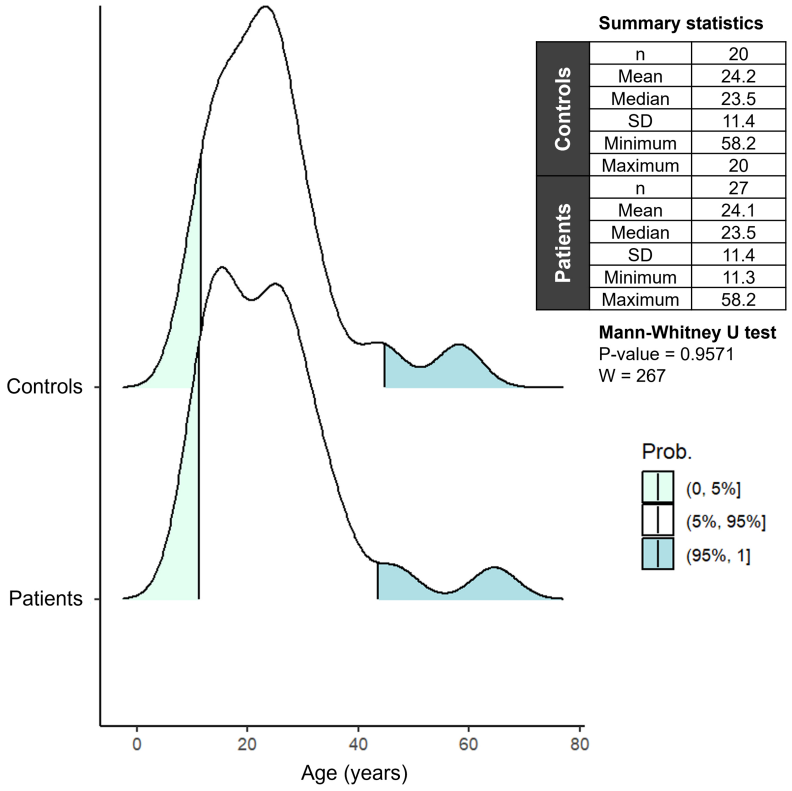


Figure S1: Statistical comparison of age distributions of patients (27 eyes) and healthy control subjects (20 eyes) included in the analysis of retinal layer thickness. A Mann-Whitney U test confirmed no statistical difference in age between both groups.

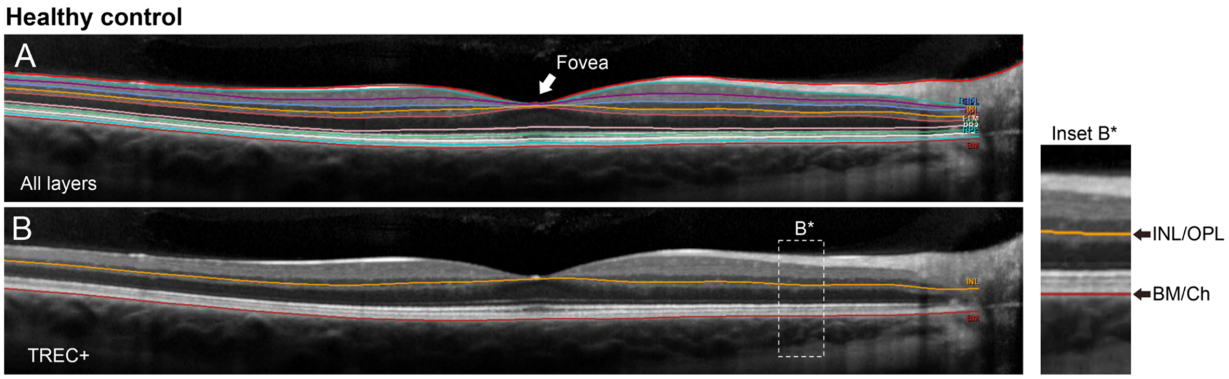


Figure S2: Semi-automated segmentation of spectral domain-optical coherence optical coherence tomography (SD-OCT) scans and thickness quantification of the total receptor+ (TREC+) layer in a healthy retina. (A) Automated segmentation of all retinal layers visible on SD-OCT was performed by the HEYEX software (Heidelberg Engineering). (B) The TREC+ layer spanning photoreceptor attributable layers are demarcated by the inner nuclear layer/outer plexiform (INL/OPL, orange line)(Inset B*) interface and Bruch's membrane/choroidal (BM/Ch, red line) interface boundaries. Mis-segmented regions were manually corrected as necessary.

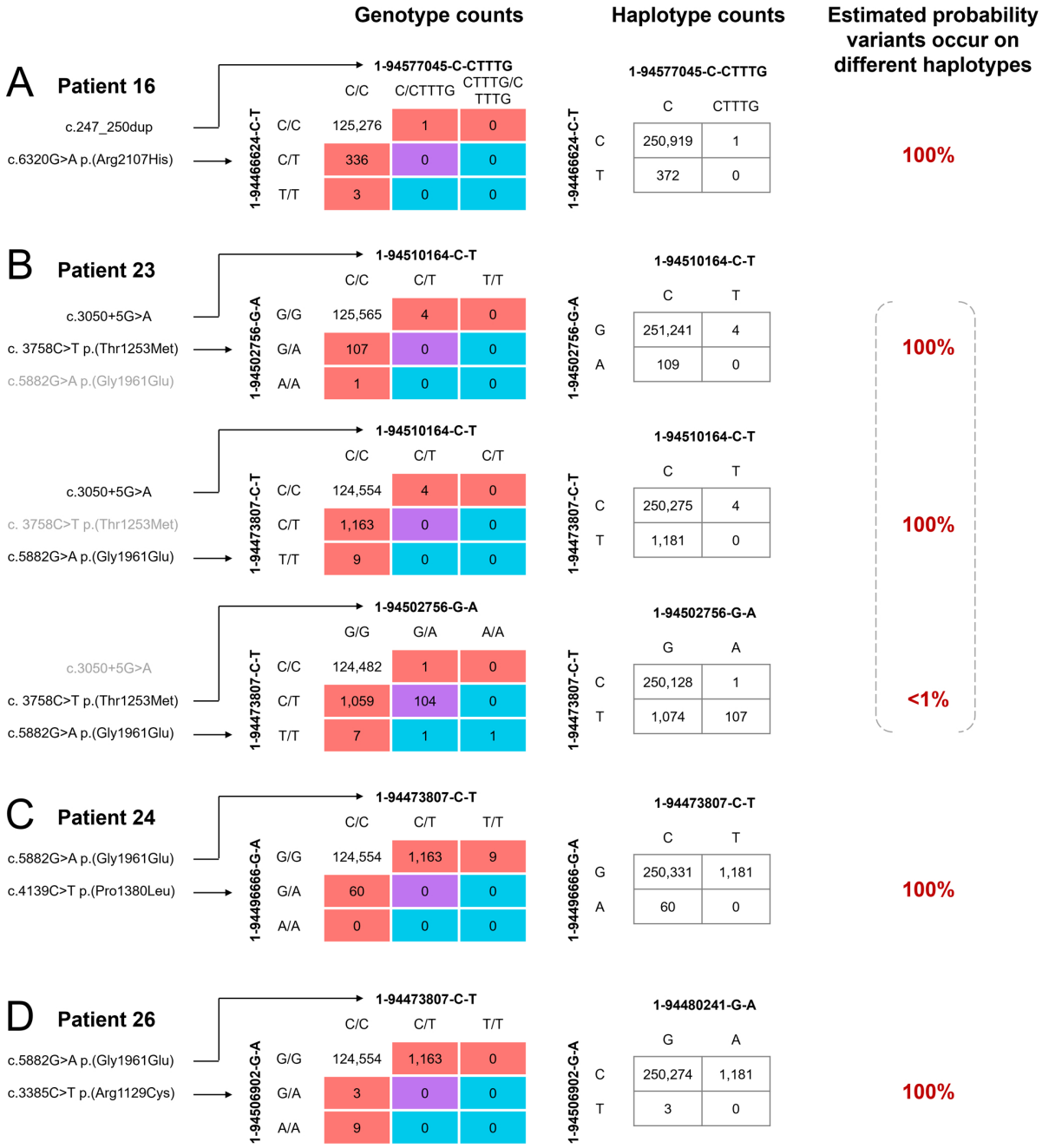


Figure S3: Analysis of co-occurrence patterns in the general population of *ABCA4* variants found in study patients in whom familial screening for phase determination was not available. Genotype counts are presented in 3x3 tables listing the number of individuals (exomes) in the gnomADv2.1.1 database with these genotype combinations. Red squares are individuals with variants falling on different haplotypes; blue squares are individuals with variants falling on the same haplotype; purple squares are indeterminant. Haplotype counts are estimated based on an expectation-maximization algorithm. Percentages are based on expectation-maximization probability distributions.

Table S1: Summary of predicted pathogenicity and classification criteria of all *ABCA4* variants identified in the study cohort.

| cDNA (NM_000350.3) | Protein | MAF | CADD | SpliceAI |
|---|---|---|---|---|
| c.6729+5_6729+19del | p.(Phe2161Cysfs*3) | 3.53E-05 | 11.4 | Donor Loss at 20 bp (Δscore = 0.96) |
| c.6449G>A | p.(Cys2150Tyr) | 2.83E-05 | 32 | - |
| c.6448T>C | p.(Cys2150Arg) | 6.84E-07 | 29.8 | - |
| c.6320G>A | p.(Arg2107His) | 2.03E-03 | 32 | - |
| c.6079C>T | p.(Leu2027Phe) | 4.99E-04 | 28.5 | - |
| c.5882G>A | p.(Gly1961Glu) | 3.44E-03 | 28.4 | - |
| c.5318C>T | p.(Ala1773Val) | 2.74E-05 | 28.7 | - |
| c.5196+1056A>G | p.(Met1733Valfs*2) | (not found) | - | Cryptic Donor Strongly activated |
| c.5196+1G>A | p.(?) | 2.55E-05 | 33 | Donor Loss at 1 bp (Δscore = 0.99) |
| c.5044_5058del | p.(Val1682_Val1686del) | 6.16E-06 | - | No significant effect |
| c.4947del | p.(Glu1650Argfs*12) | 3.42E-06 | - | Acceptor Loss at 99 bp (Δscore = 0.24) |
| c.4253+4C>T | p.(Ile1377Hisfs*3) | 1.29E-05 | - | Donor Loss at 4 bp (Δscore = 0.19) |
| c.4234C>T | p.(Gln1412*) | 1.98E-05 | 51 | - |
| c.4139C>T | p.(Pro1380Leu) | 2.93E-04 | 25.2 | - |
| c.3413T>A | p.(Leu1138His) | 1.37E-06 | 29.4 | - |
| c.3385C>T | p.(Arg1129Cys) | 1.50E-05 | 29.1 | - |
| c.3335C>A | p.(Thr1112Asn) | 1.50E-05 | 26.6 | Close to Exon 23 boundary; possible splice defect |
| c.3292C>T | p.(Arg1098Cys) | 2.46E-05 | 29.1 | - |
| c.3065A>G | p.(Glu1022Gly) | (not found) | 32 | - |
| c.3050+5G>A | p.(Leu973_His1017delinsPhe) | 1.59E-05 | - | Donor Loss at 5 bp (Δscore = 0.89) |
| c.2971G>C | p.(Gly991Arg) | 2.64E-04 | 28.7 | - |
| c.2966T>C | p.(Val989Ala) | 8.35E-05 | 23.5 | - |
| c.2918+5G>A | p.(Glu921Profs*3) | (not found) | - | Donor Loss at 5 bp (Δscore = 0.98) |
| c.2461T>A | p.(Trp821Arg) | 7.52E-06 | 28.6 | - |
| c.1844T>C | p.(Val615Ala) | (not found) | 23.7 | - |
| c.634C>T | p.(Arg212Cys) | 1.18E-04 | 29.6 | - |
| c.247_250dup | p.(Ser84Thrfs*16) | 6.57E-06 | 25.4 | No significant effect |
| c.45G>A | p.(Trp15*) | 1.37E-06 | 39 | - |
| c.[5461-10T>C;5603A>T] | p.([Thr1821Aspfs*6,Thr1821Valfs*13;Asn1868Ile]) | - | - | - |
| c.[2588G>C;5603A>T] | p.([Gly863Ala, Gly863del;Asn1868Ile]) | - | - | - |
| c.[3758C>T;5882G>A] | p.([Thr1253Met;Gly1961Glu]) | - | - | - |
| c.[1622T>C;3113C>T] | p.([Leu541Pro;Ala1038Val]) | - | - | - |
| c.[769-784C>T;5882G>A] | p.([Leu257Aspfs*3,Gly1961Glu]) | - | - | - |